Mem. S.A.It. Suppl. Vol. 19, 237

Memorie della
Supplementi

NIR luminosity functions and stellar mass functions of galaxies in the Shapley supercluster environment

A. Mercurio[1], P. Merluzzi[1], C. P. Haines[2], R. J. Smith[3], G. Busarello[1], and J. R. Lucey[3]

[1] Istituto Nazionale di Astrofisica – Osservatorio Astronomico di Napoli, Italy
[2] School of Physics and Astronomy, University of Birmingham, Birmingham B15 2TT
[3] Department of Physics, University of Durham, Durham DH1 3LE

Abstract. We present the near-infrared (NIR) luminosity and stellar mass functions of galaxies in the core of the Shapley supercluster at z=0.048 based on the new *K*-band observations carried out at the United Kingdom Infra-Red Telescope with the Wide Field Infrared Camera in conjunction with B- and R-band photometry from the Shapley Optical Survey. We examine environmental effects on galaxy properties, showing both luminosity (LFs) and stellar mass functions (SMFs) in three regions selected according to the local galaxy density. We find different behaviours of the LF and the galaxy SMF with the environment suggesting that the mechanisms transforming galaxies in different environments are related to the quench of star-formation rather than to mass-loss.

Key words. Galaxies: clusters: general — Galaxies: clusters: individual: Shapley supercluster — Galaxies: photometry — Galaxies: luminosity function — Galaxies: stellar content — Galaxies: evolution

1. Introduction

The properties and evolution of galaxies are strongly related to their environment (e.g. Treu et al. 2003; Baldry et al. 2006). In the local universe this environmental dependence has been investigated and observed in the distribution of galaxy luminosities and stellar masses, providing constraints on the assembly of galaxies over cosmic time. Since the NIR light is dominated by established old stellar populations rather than by recent star-formation activity, the NIR LF can be considered as a reliable estimator of the SMF (Gavazzi et al. 1996; Bell & de Jong 2001) and the shape of the NIR LF constrains the scenarios of galaxy formation (e.g. Benson et al. 2003).

In this context we study the *K*-band LF of the Shapley supercluster core (SSC) down to the dwarf regime (reaching $\sim M^{\star}+6$) with the aim of i) quantifying the environmental impact on the shape of the NIR LF; ii) deriving the stellar masses of the supercluster galaxies; iii) investigating the mechanisms driving galaxy evolution as a function of the galaxy mass. This work is carried out in the framework of the joint research programme ACCESS [1] (*A*

Send offprint requests to: A. Mercurio
e-mail: mercurio@na.astro.it

[1] http://www.oacn.inaf.it/ACCESS

Complete Census of Star-formation and nuclear activity in the Shapley supercluster, PI: P. Merluzzi) aimed at determining the importance of cluster assembly processes in driving the evolution of galaxies as a function of the galaxy mass and environment within the Shapley supercluster.

2. NIR Luminosity Functions in different environments

We analysed new near-infrared complemented by panoramic *B*- and *R*-band imaging from the Shapley Optical Survey (SOS, see Mercurio et al. 2006 and Haines et al. 2006 for details). In Fig. 1 the optical and NIR survey are superimposed.

The *K*-band survey of the SSC was carried out at the United Kingdom Infra-Red Telescope (UKIRT) with the Wide Field Infrared Camera (WFCAM) in April 2007. We observed a total area of 3.043 deg^2 (of which ∼2 deg^2 overlap with the SOS) covering three Abell clusters A3556, A3558 and A3562 and two poor clusters SC 1327-312 and SC 1329-314, as shown in Fig. 1. The total exposure time for each field is 300 s, reaching K=19.5 mag at 5σ, with typical FWHMs of 0.9-1.2 arcsec (see Merluzzi et al. 2010 for details).

The *K*-band galaxy LF of the SSC has been derived down to the magnitude limit K=18 mag accounting for interlopers by the statistical subtraction of the background contamination.

The number counts in the supercluster field has been obtained by weighting each galaxy's contribution to a given magnitude bin according to its completeness. We also correct for the contamination of the misclassified stars.

The background contamination was estimated through three control fields from the UKIRT Infrared Deep Sky Survey (UKIDSS) Deep Extragalactic Survey (DXS) (Lawrence et al. 2007). We subtracted the control field counts from those obtained in the Shapley area in order to obtain supercluster member counts. Following Bernstein et al. (1995) the background counts are estimated as the mean of the control field counts corrected for the ratio between the observed areas (Eq. 1 of Bernstein et al. 1995) and errors on the background counts are estimated through an empirical approach as the *rms* of the counts in each control field with respect to the mean estimated over the whole area (Eq. 2 of Bernstein et al. 1995).

In order to investigate the effects of the environment on galaxy properties, we derived and compared the LFs in three different regions of the supercluster, characterised by high-, intermediate- and low-densities of galaxies (see Fig. 1) where galaxy densities are ρ >1.5, 1.0< ρ ≤1.5 and 0.5< ρ ≤1.0 gals arcmin^{-2}, respectively. The local density of R < 21 mag galaxies, Σ, was determined across the *R*-band WFI mosaic (i.e. in a 2 deg^2 area, see Fig. 1). We derive Σ by using an adaptive kernel estimator (Pisani 1993; 1996), in which each galaxy i is represented by a Gaussian kernel, $K(r_i) \propto \exp(-r^2/2\sigma_i^2)$, whose width σ_i is proportional to $\Sigma_i^{-1/2}$ thus matching the resolution locally to the density (see Mercurio et al. 2006 for more details).

In Fig. 2, we show the *K*-band LFs of galaxies in the high- (black), intermediate- (red) and low-density (blue) regions covering areas (in the SOS/*K*-band survey overlap) of ∼0.115, 0.330 and 1.062 deg^2, respectively, together with their fits with a Schechter function (same colour code). The background subtraction was performed scaling the counts with the area values because of the complex geometry of the three density regions. Figure 3 shows the confidence contours of the best fitting Schechter function for the three density regions. The faint-end slope becomes steeper from high- to low-density environments varying from –1.33 to –1.49, being inconsistent at the 2σ confidence level (c.l.) between high- and low-density regions.

According to the χ^2 statistics, in all the three environments the fit with a single Schechter function cannot be rejected, but there is some "structure" evident in the residuals: the fit systematically under- and over-predicts the observed counts as a function of the magnitude. The LFs suggest instead a bimodal behaviour due to the presence of an upturn for faint galaxies, that cannot be described by using a single Schechter function.

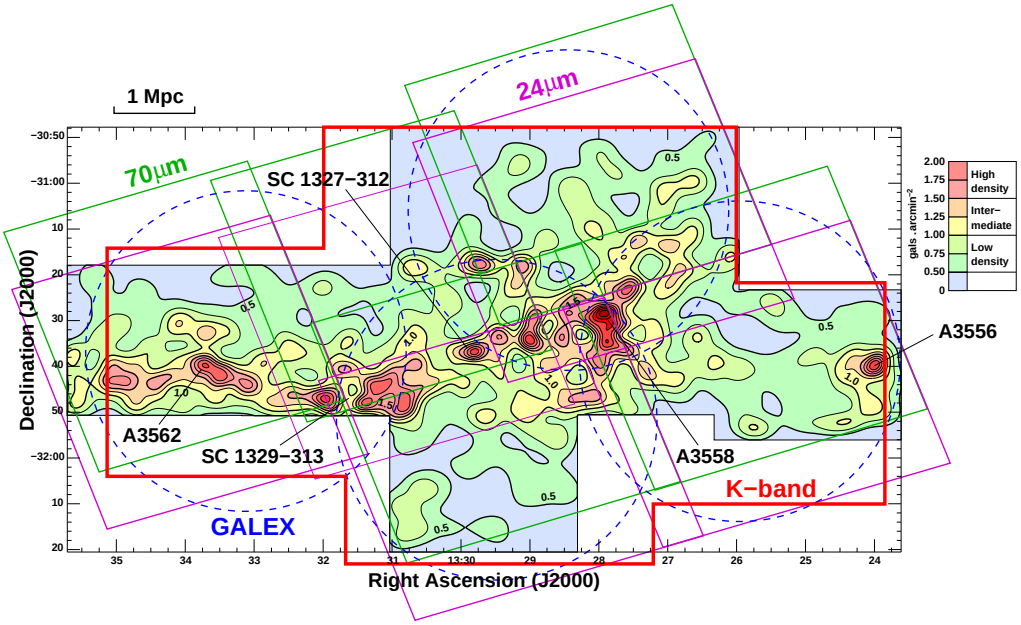

Fig. 1. The Shapley NIR survey (thick red) is shown superimposed to the surface density of R < 21.0 galaxies as derived from the SOS (see text). Isodensity contours are shown at intervals of 0.25 galaxies arcmin^{-2}, with the thick contours corresponding to 0.5, 1.0 and 1.5 galaxies arcmin^{-2}, the densities used to separate the three cluster environments. The multi-wavelength photometric coverage of ACCESS on the SSC are also shown. Magenta: 24 μm, green: 70 μm, blue dashed: 150 nm and 250 nm.

Table 1. Fits to the LFs. Errors on the m* and α parameters can be obtained from the confidence contours shown in Fig. 3. Column 1: the analyzed region. Columns 2 and 3: characteristic magnitude of the Schechter function (apparent m* and absolute M*). Column 4: the value of slope α. Columns 5 and 6: reduced χ^2 and its probability P($\chi^2 > \chi^2_\nu$).

Region	m*	M*	α	χ^2_ν	P
high density	11.48	−25.18	−1.33	0.77	69.31%
int density	11.47	−25.19	−1.44	1.30	20.39%
low density	11.51	−25.15	−1.49	1.00	44.78%

In order to investigate the processes responsible for changing the shape of the galaxy LF, we compare the trends observed for the optical and the NIR LFs. Since the NIR LF is expected to approximate the SMF, while the optical LFs are more sensitive to the galaxy star-formation history, both are needed for investigating the nature of galaxies which dominate the faint-end. For instance, a steep optical LF can be compatible with a flat SMF if dwarf galaxies have their luminosities boosted by starbursts, a scenario which can be probed by comparison to the NIR LF.

The optical LF of the SSC derived in the SOS (see Mercurio et al. 2006) cannot be described by a single Schechter function due to the dips apparent at M*+2 both in B and R bands and the clear upturn in the counts for galaxies fainter than B and R ∼18 mag. Instead the sum of a Gaussian and a Schechter function, for bright and faint galaxies, respectively, is a suitable representation of the data. Furthermore, the slope values becomes significantly steeper from high- to low-density environments varying from –1.46 to –1.66 in B

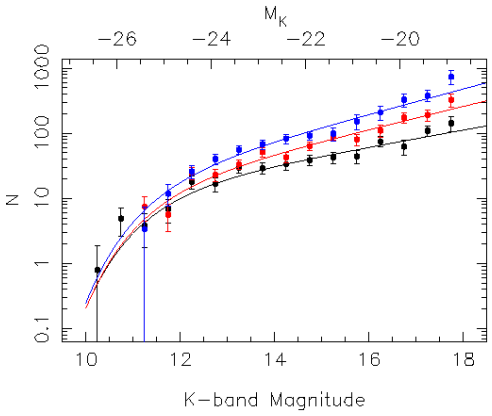

Fig. 2. K-band LFs of galaxies in the three cluster regions corresponding to high- (black), intermediate- (red) and low-density (blue) environments. The continuous lines represent the fits with Schechter function. The counts are per half magnitude bin.

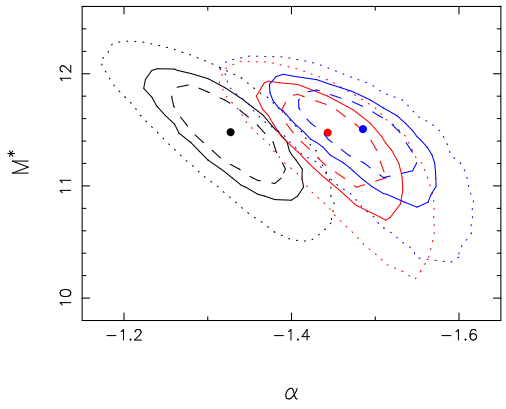

Fig. 3. 1 (dashed contours), 2 (solid) and 3σ (dotted) confidence levels for the K-band Schechter parameters (Fig. 2) in the three cluster regions corresponding to high- (black), intermediate- (red) and low-density (blue) environments.

band and from −1.30 to −1.80 in R band, being inconsistent at more than 3σ c.l. in both bands. Such a marked luminosity segregation is related to the behaviour of the red galaxy population: while red sequence counts are very similar to those obtained for the global galaxy population, the blue galaxy LFs are well described by single Schechter functions and do not vary with the density (see Mercurio et al. 2006). This suggests that mechanisms transforming galaxies in different environments are mainly related to the quench of star-formation.

3. The galaxy stellar mass functions

The combined optical and NIR data allow us to derive the distribution of galaxy stellar masses. The sample we analysed is in the magnitude range $10 \leq K \leq 18$ and refers to the $\sim$2 deg^2 area covered by both the SOS and our K-band imaging. We note that although the area of the NIR survey is slightly different from that of the SOS, both surveys map the same kinds of environment from the low- to the high-density (see the isodensity contours in Fig. 1).

The stellar masses ($\mathcal{M}$) of galaxies belonging to the SSC are estimated by means of stellar population models constrained by the observed optical and infrared colours. It is well known that stellar masses estimated using the fit to the multicolour spectral energy distribution (SED) are model dependent and subject to various degeneracies. In order to reduce such degeneracies we have used a large grid of complex stellar population models by Maraston (2005) with a Salpeter initial mass function covering a wide range of parameters. We use SEDs with the star-formation history (SFH) parameterised as $\Psi(t) \propto \exp(-t/\tau)$, with τ between 1.0 and 20.0 Gyr, ages between 0.001 and 14 Gyr and metallicities in the range 0.5-2.0 $Z_\odot$. The synthetic spectra are shifted to the galaxy spectroscopic redshift, if known, or at the median supercluster redshift z=0.05. Then for each of them we compute the B, R and K magnitudes by adopting the Calzetti (2001) extinction. The most appropriate evolutionary history is selected by fitting the optical + NIR photometry, and the mass is estimated by normalising the best-fit SED to the observed K-band magnitude.

We use the probability that galaxies are supercluster members as derived by Haines et al. 2006 following Kodama & Bower (2001) in order to estimate and correct for the foreground/background contamination. Although there exists about 650 galaxy redshifts in the region covered by optical and NIR photometry, corresponding to $\sim$ 90 % of $R < 16$ mag

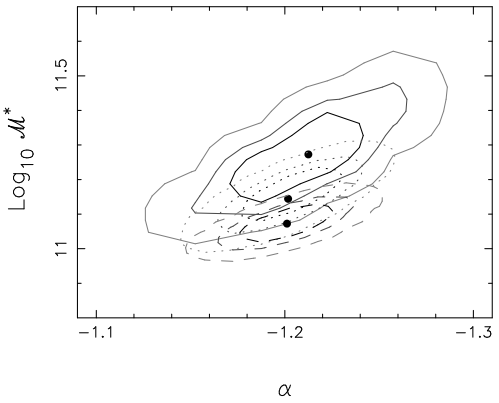

Fig. 5. The 1, 2 and 3σ confidence levels for the Galaxy SMF parameters in the three cluster regions corresponding to high- (solid contours), intermediate- (dotted) and low-density (dashed) environments.

galaxies, we need to adopt a complementary approach for those galaxies without spectroscopic information and to extend the magnitude range. For this reason we choose that stellar masses of galaxies belonging to the Shapley supercluster contribute to the galaxy SMF according to their likelihood of belonging to the SSC.

In Fig. 4 we show the SMF for the different supercluster environments. Unlikely in the case of the LF no environmental trend is seen in the slope of the SMFs (see Fig. 5). On the other hand, the $\mathcal{M}^\star$ increase from low- to high-density regions and the excess of high-mass galaxies remains dependent on the environment. The different behaviours of LF and of galaxy SMF with the environment confirm that the mechanisms transforming galaxies in different environments are mainly related to the quench of star-formation rather than to mass-loss.

4. Summary and conclusions

It is well known that the NIR luminosities provide a more reliable estimate of the stellar masses compared to the optical ones due to the fact that the mass-to-light ratios in the NIR vary by at most a factor 2 across a wide range of star formation histories (Bell & de Jong 2001) in comparison to the much larger variations of the M/L ratios (up to a factor 10) observed at optical wavelengths. In addition the effects of the extinction are much weaker at infrared wavelengths that in the optical ones, and k-corrections for infrared colours are only weakly dependent on the Hubble type and vary slowly with redshift (e.g. Poggianti 1997). In our study we exploit new deep (K=18 mag) K-band imaging of the SSC complemented by the deep optical imaging down to B=22.5 mag and R=22 mag from the SOS, and a spectroscopically confirmed supercluster sample of ~650 galaxies across the same field which is ~90% complete at R <16 mag. We present an analysis of the K-band LF of galaxies as a function environment and we derive the galaxy SMF in order to constrain the physical mechanisms that transform galaxies in different environments as a function of the galaxy mass.

We find that the K-band LF faint-end slope becomes steeper from high- to low-density environments varying from –1.33 to –1.49, being inconsistent at the 2σ c.l. (see Tab 1), indicating that the faint galaxy population increases in low-density environments. Such an environmental dependence confirms our finding for the optical LFs derived in the same supercluster regions although the changes in slope are less dramatic at NIR wavebands. Differently from the LF no environment effect is found in the slope of the SMFs. On the other hand, the $\mathcal{M}^\star$ increase from low- to high-density regions and the excess of galaxies at the bright-end is also dependent on the environment. This trend is in general agreement with the results of Baldry et al. (2006).

By comparing the effect of environment at optical and NIR wavebands in shaping the LFs and taking into account that the slope of the galaxy SMF is invariant with respect to the environment, it seems that the physical mechanism responsible for the transformation of galaxies properties in different environment are related to the quenching of the SF. This suggests that the mechanism responsible for shaping the LF and SMF is partially related to the mass loss due to tidal stripping or galaxy harassment, but gas stripping by the ICM can also affect the galaxy population removing the cold

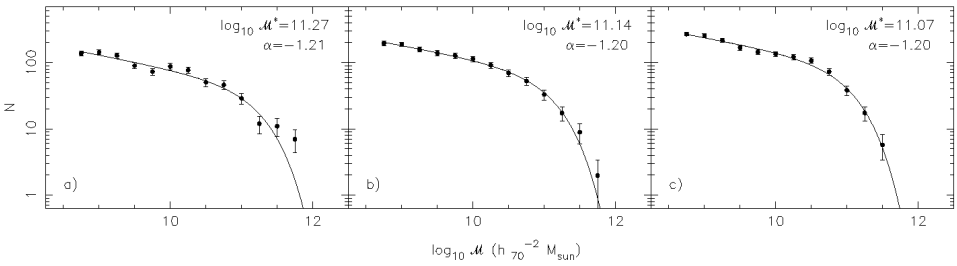

Fig. 4. The mass function of galaxies in the three cluster regions corresponding to high- (panel a) , intermediate- (panel b) and low-density (panel c) environments. In the left, central and right panel the continuous line represents the fit to the data. In each panel the best fit value of α and $\log_{10}$ M* are reported.

gas supply and thus rapidly terminating ongoing star-formation. These mechanisms all require a dense ICM and so their evolutionary effects on massive galaxies are limited to the cores of clusters, but can extend to poorer environments for dwarf galaxies which are easier to strip. The infalling galaxies are probably late-type (see Mercurio et al. 2006) that are affected by gas stripping entering in the supercluster. On the other hand, the depth of the NIR survey could affect the present results by not allowing us to detect an upturn of the SMF which can be detected at a mass range lower than reached here (see Jenkins et al. 2007). In order to identify the mechanisms which drive galaxy evolution in the supercluster environment we are undertaking a survey with the integral field spectrograph WiFeS which will provide a unique data set to investigate in details the stellar populations and kinematics for a subsample of the Shapley galaxies.

Acknowledgements. This work was carried out in the framework of the FP7-PEOPLE-IRSES-2008 project ACCESS. AM acknowledges financial support from INAF-OAC. The authors wish to thank the staff at UKIRT, CASU and WFAU for making observations and processing data, and the UKIDSS project and archive which has been used for the field galaxy counts.

References

Baldry I. K., et al., 2006, MNRAS, 373, 469
Bell E. F., de Jong R. S., 2001, ApJ, 550, 212
Benson A. J., et al., 2003, ApJ, 599, 38
Bernstein G. M., et al., 1995, AJ, 110, 1507
Calzetti D., 2001, PASP, 113, 1449
Gavazzi G., Pierini D., Boselli A., 1996, A&A, 312, 397
Haines C. P., et al., 2006, MNRAS, 371, 55
Jenkins L. P., et al., 2007, AJ, 666, 846
Kodama T., Bower R., 2001, MNRAS, 321, 18
Lawrence A., et al., 2007, MNRAS, 379, 1599
Maraston C., 2005, MNRAS, 362, 799
Mercurio A., et al., 2006, MNRAS, 368, 109
Merluzzi P., et al., 2010, MNRAS, 402, 753
Pisani A., 1993, MNRAS, 265, 706
Pisani A., 1996, MNRAS, 278, 697
Poggianti B. M., 1997, A&AS, 122, 399
Treu T., et al., 2003, ApJ, 591, 53